JACS
JOURNAL OF THE AMERICAN CHEMICAL SOCIETY

pubs.acs.org/JACS

Article

Switchable Catalysis Improves the Properties of CO_2-Derived Polymers: Poly(cyclohexene carbonate-*b*-ε-decalactone-*b*-cyclohexene carbonate) Adhesives, Elastomers, and Toughened Plastics

Gregory S. Sulley, Georgina L. Gregory, Thomas T. D. Chen, Leticia Peña Carrodeguas, Gemma Trott, Alba Santmarti, Koon-Yang Lee, Nicholas J. Terrill, and Charlotte K. Williams*

Cite This: *J. Am. Chem. Soc.* 2020, 142, 4367−4378

Read Online

ACCESS | Metrics & More | Article Recommendations | Supporting Information

ABSTRACT: Carbon dioxide/epoxide copolymerization is an efficient way to add value to waste CO_2 and to reduce pollution in polymer manufacturing. Using this process to make low molar mass polycarbonate polyols is a commercially relevant route to new thermosets and polyurethanes. In contrast, high molar mass polycarbonates, produced from CO_2, generally under-deliver in terms of properties, and one of the most widely investigated, poly(cyclohexene carbonate), is limited by its low elongation at break and high brittleness. Here, a new catalytic polymerization process is reported that selectively and efficiently yields degradable ABA-block polymers, incorporating 6−23 wt % CO_2. The polymers are synthesized using a new, highly active organometallic heterodinuclear Zn(II)/Mg(II) catalyst applied in a one-pot procedure together with biobased ε-decalactone, cyclohexene oxide, and carbon dioxide to make a series of poly(cyclohexene carbonate-*b*-decalactone-*b*-cyclohexene carbonate) [PCHC-PDL-PCHC]. The process is highly selective (CO_2 selectivity >99% of theoretical value), allows for high monomer conversions (>90%), and yields polymers with predictable compositions, molar mass (from 38−71 kg mol^{-1}), and forms dihydroxyl telechelic chains. These new materials improve upon the properties of poly(cyclohexene carbonate) and, specifically, they show good thermal stability ($T_{d,5}$ ∼ 280 °C), high toughness (112 MJ m^{-3}), and very high elongation at break (>900%). Materials properties are improved by precisely controlling both the quantity and location of carbon dioxide in the polymer chain. Preliminary studies show that polymers are stable in aqueous environments at room temperature over months, but they are rapidly degraded upon gentle heating in an acidic environment (60 °C, toluene, *p*-toluene sulfonic acid). The process is likely generally applicable to many other lactones, lactides, anhydrides, epoxides, and heterocumulenes and sets the scene for a host of new applications for CO_2-derived polymers.

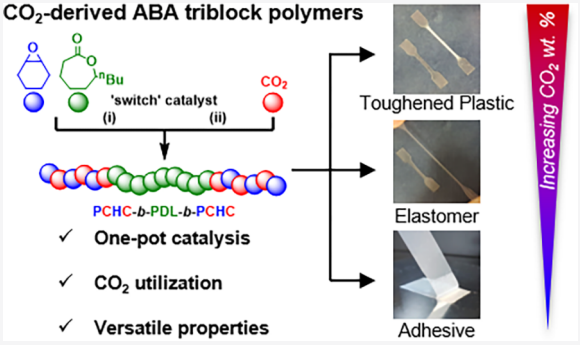

INTRODUCTION

Devising methods to efficiently use carbon dioxide in chemical synthesis is a fundamentally important challenge.[1−4] The ring opening copolymerization (ROCOP) of carbon dioxide and epoxides is a truly catalytic process that enables high CO_2 uptake and allows for the partial substitution of polluting and costly petrochemicals (epoxides) with cheaper carbon dioxide.[5,6] Current academic and industrial research focuses on applying ROCOP to make low molar mass (M_n) poly(carbonate/ether carbonate) polyols, i.e., chains with M_n = 1−10 kg mol^{-1} and hydroxyl chain-end groups.[7,8] These CO_2-polyols deliver high-performance thermosets or polyurethanes that are used to make flexible foams for furniture, rigid foams for home insulation, scratch-resistant coatings, and thermoplastic polyurethanes.[8−14] Life cycle analysis comparing CO_2-polyols with industrially used polyether polyols, made using 100% epoxide, shows a triple win in terms of greenhouse gas emissions: for every molecule of CO_2 polymerized, two more molecules are saved in avoiding epoxide usage.[15] Other reports describe how to integrate CO_2/epoxide ROCOP with industrial CO_2 capture technologies.[3,16]

Carbon dioxide/epoxide ROCOP can also deliver high molar mass polycarbonates (M_n = 10−100 kg/mol^{-1}) and among the most widely synthesized is poly(cyclohexene carbonate) (PCHC).[17,18] There are many reports of catalysts delivering PCHC, from CO_2/cyclohexene oxide (CHO) ROCOP; the highest performing are dinuclear metal complexes or bicomponent metal complex and cocatalyst

Received: December 5, 2019
Published: February 20, 2020

https://dx.doi.org/10.1021/jacs.9b13106
J. Am. Chem. Soc. 2020, 142, 4367−4378

systems.[19,20] Our research group has developed macrocyclic dinuclear catalysts that operate at 1 bar carbon dioxide pressure, and the most active are heterodinuclear Zn(II)/Mg(II) complexes.[21−25] Despite the many advances in catalyst development, there is a paucity of reports addressing the properties and applications for PCHC. Nearly 20 years ago, Koning et al. reported that PCHC has a high glass transition temperature (105−115 °C), high stress at break (11−42 MPa), and excellent tensile modulus (2400−3600 MPa), but is limited by a very low elongation at break (0.5−2%) and by its brittleness.[26,27] Others noted its thermal decomposition temperature can be very low (<200 °C), which may cause processing difficulties.[28] Since this time, material development has been limited and any current application of PCHC necessitates plasticizers and additives to overcome its brittleness. One strategy to improve the properties of PCHC, and more generally CO_2-polycarbonates, is to incorporate them into block polymers. Although there are reports of the syntheses of copolymers of PCHC with petroleum derived blocks, e.g., poly(acrylates), -ethers, -styrenes, -vinyl ethers, and -siloxanes, none investigate the resulting materials properties.[29−33] This may be due, in part, to the overall copolymer molar masses being too low (M_n < 20 kg mol^{-1}) to allow for block phase separation and, hence, the compromised mechanical performances. Also, these copolymers combine a CO_2-polycarbonate with a nondegradable petrochemical, raising questions about end-of-life fate.

Combining a CO_2-polycarbonate and polyester in a block polymer could be better from the sustainability point of view since both blocks are degradable and many of the raw materials could be renewably sourced.[34−36] In 2014, our group reported switchable catalysis whereby a single metal catalyst is "switched" between CO_2/epoxide ROCOP and lactone ring-opening polymerization (ROP) cycles allowing a one-pot route to poly(ester-*b*-carbonates) (Scheme 1).[37] Switchable catalysis has subsequently been applied to other catalysts and monomers allowing production of various block polyesters, -carbonates, and ethers.[38−50] Most of these prior reports have focused on understanding and improving the catalysis with little investigation of the polymer properties. Very recently, Rieger and co-workers applied switchable catalysis to make block and statistical copolymers of poly(β-butyrolactone) and PCHC.[51] The block copolymers show phase separation, and at 50 wt % PCHC content the materials' tensile elongation at break values reach 5% (PCHC = 0.5−2%). By applying a better choice of soft block material, switchable catalysis could significantly improve upon PCHC properties, but the method is still hampered by several catalyst and process limitations. First, the switchable catalytic rates are still too low; for example, under monomer mixture conditions CO_2/epoxide ROCOP TOFs are 1−50 h^{-1} and lactone ROP values are 1−100 h^{-1}.[37,40,51] Second, when producing higher molar mass block polymers, there are difficulties controlling the chain end groups, which leads to mixtures of structures (vide infra). Third, the overall block polymer molar masses are too low for block phase separation, which limits the resulting thermal-mechanical properties.

Scheme 1. Catalytic Cycles Accessed by a Single, Switchable Catalyst for ABA Triblock Polymers

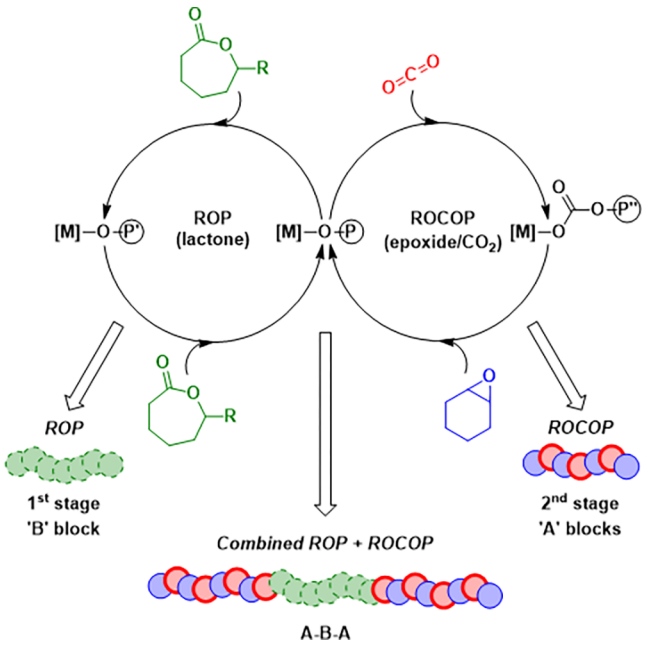

To address these barriers, a new catalyst selective for the production of high molar mass ABA block polymers, featuring poly(cyclohexene carbonate) (PCHC) as the A block and poly(ε-decalactone) (PDL) as the B block, is proposed. The block combination is designed so that the rigid structure of PCHC, together with its high glass transition temperature (T_g ∼ 110−120 °C), serves as a "hard" block and benefits the resulting material with a high tensile modulus.[26,27] To accompany it, PDL is a useful "soft" block due to its amorphous structure, low T_g (−60 °C) and relatively low entanglement molar mass.[46] The polymers are also designed to increase the biobased content, as ε-decalactone is sourced from plants and CO_2 is a common byproduct of bioprocessing, as well as being a common industrial waste.[16,46] CHO is currently sourced from petroleum, but routes from fatty acid coproducts could be implemented to increase biobased content.[52] Finally, by combining carbonate and ester blocks, obviating plasticizer usage, it is envisaged that (chemical) recycling will be facilitated, while the rigid and substituted main chain structures should provide the balance of sufficient material stability.

RESULTS

To prepare the new ABA triblock polymers, it is essential to overcome catalyst activity limitations, to control chain end-groups, and to deliver high molar mass polymers (M_n > 50 kg mol^{-1}). To apply a one-pot switchable procedure, a single catalyst that can be directed between the CHO/CO_2 ROCOP and ε-DL ROP cycles is needed (Scheme 1). To increase the catalytic rates, a Zn(II)/Mg(II) catalyst, featuring *para*-di(methyl)amino-benzoate coligands, is selected as it shows some of the highest absolute rates in CHO/CO_2 ROCOP, especially at 1 bar pressure (Figure 1).[21] First it is necessary to evaluate the catalytic performance in lactone ROP. It is essential to solve a well-known problem affecting epoxide/CO_2 ROCOP: most catalysts deliver a mixture of α,ω-dihydroxyl telechelic and α-hydroxyl-ω-carboxylate end-capped polymer chains, observed through bimodal molar mass distributions and by end-group analysis.[53−55]

The mixed chain end-groups arise because the copolymerization is initiated both from the catalyst (e.g., from the benzoate coligand) and from diols (e.g., 1,2-cyclohexane diol, CHD); the diols either contaminate the epoxide or are rapidly formed upon reaction of the epoxide with even ppm quantities

https://dx.doi.org/10.1021/jacs.9b13106
J. Am. Chem. Soc. 2020, 142, 4367−4378

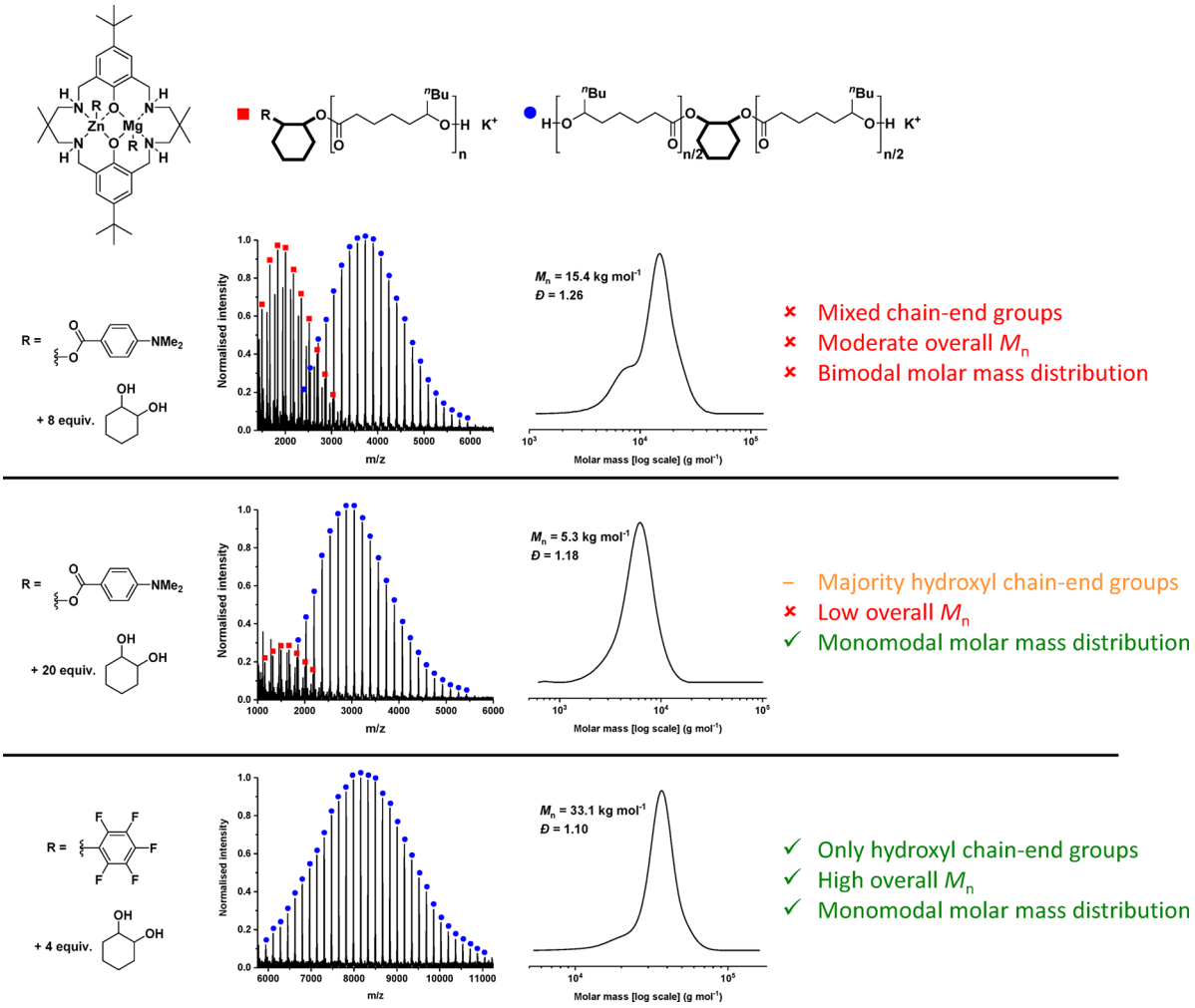

Figure 1. Ring opening polymerizations of ε-decalactone (DL) conducted using [LZnMgR$_2$]:CHD:DL:CHO = 1:x:400:1000, 0.16−1 h, 80 °C. The figure illustrates the two Zn(II)/Mg(II) catalyst structures ([LZnMgR$_2$], where R = ^{pNMe2}benzoate or R = C_6F_5). The structures of the two PDL chain end groups are illustrated together with the resulting MALDI-TOF and SEC data (N.B., molar mass values for SEC and MALDI-TOF differ because different samples were analyzed by each technique, see SI for further details and experimental conditions for MALDI-TOF experiments). Top: Reaction conducted using [LZnMgR$_2$], where R = ^{pNMe2}benzoate and with x = 8 (i.e., 8 equiv of CHD). Middle: Reaction conducted using [LZnMgR$_2$], where R = ^{pNMe2}benzoate and with x = 20 (i.e., 20 equiv of CHD). Bottom: Reaction conducted using [LZnMgR$_2$], where R = C_6F_5 and with x = 4 (i.e., 4 equiv of CHD).

of water (see Scheme S1 for illustrations of the ROCOP initiation and chain transfer reactions).[56] The problem is exacerbated when using catalyst + cocatalyst systems because additives like PPNCl may also initiate chains; fortunately this is obviated using the Zn(II)/Mg(II) catalyst because it functions without cocatalyst. Unsolved, the mixed end-group phenomenon would be problematic because the desired ABA polymers would be contaminated by AB type PCHC-PDL chains.

One method to suppress the catalyst initiated polymer chains is to carry out polymerizations in the presence of excess diol, e.g., 1,2-cyclohexane diol (CHD), or with additional water present. The diol is an efficient chain transfer agent and increases the quantity of α,ω-hydroxyl telechelic chains (Scheme S1). It was already observed that monomodal molar mass distributions were observed in CHO/CO_2 ROCOP when the catalyst:CHD ratio exceeded 1:8.[21] To assess the applicability of the strategy to lactone ROP, ε-DL polymerization was conducted in excess CHO as solvent, to mimic subsequent switch catalysis conditions, and using a ratio of Zn/Mg:CHD of 1:8. Under these conditions, poly(ε-decalactone) (PDL) was efficiently prepared, but it showed a bimodal molar mass distribution, by SEC analysis, and mixed chain end-groups, by MALDI-TOF mass spectrometry (Figure 1, top). Polymerizations conducted using a greater quantity of CHD (Zn/Mg: CHD = 1:20) resulted in PDL showing a monomodal molar mass distribution (Figure 1, middle). The majority of chains were dihydroxyl telechelic but the overall molar mass was very much reduced (M_n = 5.3 kg mol^{-1}), consistent with the controlled polymerization mechanism. It is clear that the strategy of adding progressively greater quantities of diol is not at all suitable for the delivery of high molar mass polymers.

An alternative approach is to prepare a catalyst featuring a labile, organometallic ligand, such as an alkyl or aryl group, that reacts with diol in situ to form the metal-alkoxide initiator.[32,49,57] One benefit could be that fewer equivalents of diol (vs catalyst) are needed to deliver effective catalysis and higher molar mass polymers are feasible. To test the hypothesis, a new Zn(II)/Mg(II) catalyst featuring two pentafluorophenyl coligands was prepared via a two-step

https://dx.doi.org/10.1021/jacs.9b13106
J. Am. Chem. Soc. 2020, 142, 4367−4378

Scheme 2. One-Pot Switchable Catalysis Synthesis of ABA (PCHC-*b*-PDL-*b*-PCHC) Triblock Polymers[a,b]

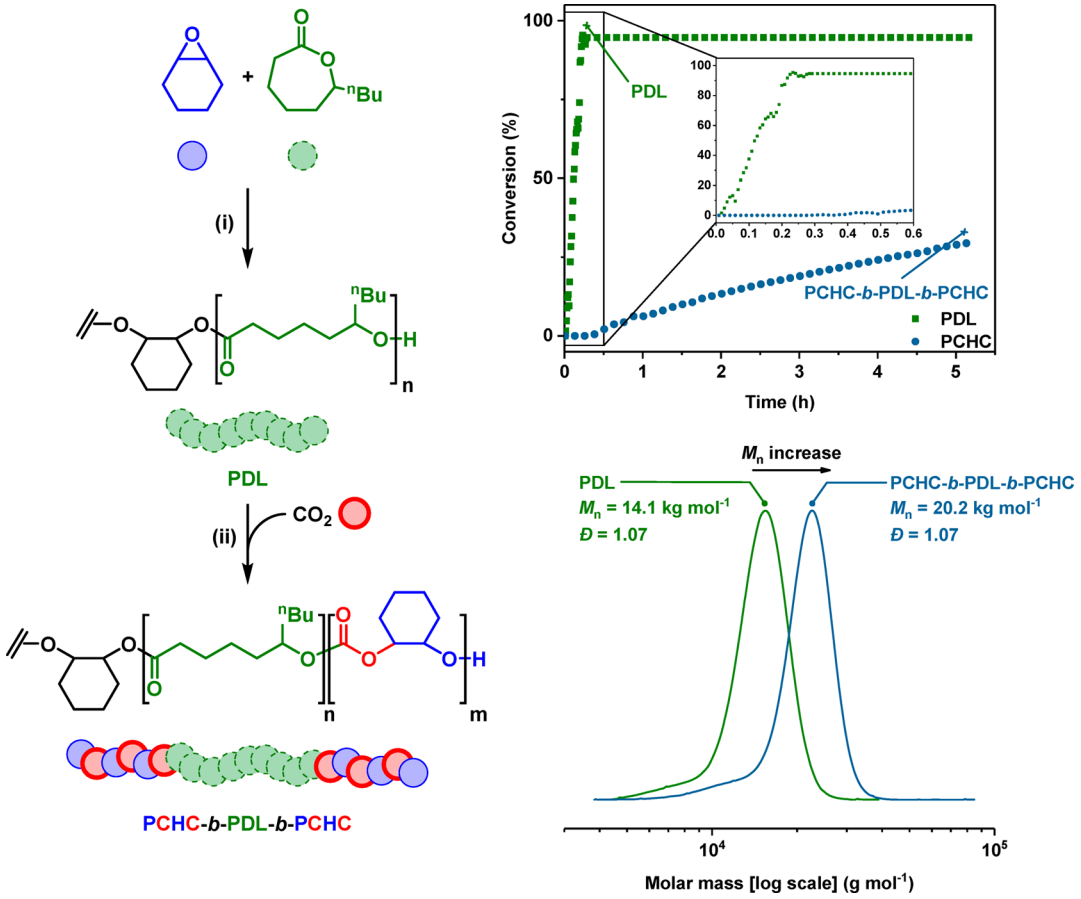

[a]Reaction conditions: (i) [LZnMg(C_6F_5)$_2$]:CHD:*ε*-DL:CHO = 1:4:*x*:*y*, where *x* and *y* are variable amounts of the two monomers for the desired block compositions, [CHO]$_0$ ~ 3 M in toluene, 80 °C, 20 min. (ii) CO_2 (20 bar), 80 °C, 20 h. *n* = *x*/2, *m* = *y*/2. Note that the conversion vs time and SEC data are collected for runs conducted using 1 bar pressure of CO_2. [b]The scheme shows conversion vs time data collected using in situ ATR-IR spectroscopy and SEC data for aliquots removed as the reaction progresses.

Table 1. PCHC-*b*-PDL-*b*-PCHC (ABA Triblock) Characterization Data

polymer[a,b]	wt % PDL:PCHC[c]	DP PDL:PCHC[d]	M_n[e] (kg mol^{-1}) [$Đ$][f]	$T_{g,DSC}$[g] (°C)	$T_{g,DMTA}$[h] (°C)	$T_{d,5\%}$[i] (°C)
ABA-20	80:20	232:68	55.9 [1.16]	−48	n.d.	286
ABA-26	74:26	307:131	71.9 [1.16]	−50	69	290
ABA-28	72:28	200:93	46.4 [1.07]	−48	n.d.	272
ABA-40	60:40	168:135	49.4 [1.08]	−49	110	278
ABA-50	50:50	147:173	59.8 [1.10]	−50; 110	118	283
ABA-76	24:76	59:225	38.0 [1.12]	−44; 81	n.d.	254

[a]ABA refers to PCHC-*b*-PDL-*b*-PCHC. See Table S1 for experimental data on monomer loading and conversion. [b]ABA-#: # denotes weight fraction of PCHC (wt %). [c]Determined by ^{1}H NMR spectroscopy using the integrals for PCHC (4.66 ppm) and PDL (4.85 ppm) (Figure S8). [d]Determined on the basis of overall monomer conversion calculated from the ^{1}H NMR spectra (See Table S2). [e]Determined by SEC, in THF, using narrow dispersity polystyrene standards. [f]M_w/M_n (Figure S12). [g]Determined by DSC analysis from the second heating cycles. T_g values reported as the midpoint of each transition (Figures S13−S18). [h]Acquired by DMTA. Upper T_g values reported as the maxima in tan(δ) (Figures S19−S22); n.d. = not determined. [i]Determined by TGA. Reported as temperature at 5% mass loss (Figures S23−S28).

synthetic procedure (see Supporting Information for full synthetic protocol and Figures S1−S6 for the characterization data).[58] The macrocyclic ligand was first reacted with 1 equiv of [Mg(N(SiMe$_3$)$_2$)$_2$] to form, in situ, the monomagnesium complex, which was then reacted with [Zn(C_6F_5)$_2$] to produce the desired [LZnMg(C_6F_5)$_2$] catalyst in good isolated yield (70%). The complex shows a sharp ^{1}H NMR spectrum, at room temperature, with eight clearly separated signals for the benzylic and methylene protons (Figure S1). This NMR feature is highly diagnostic of pure heterodinuclear complex formation, as is the observation of two mutually coupled aromatic proton signals (Figure S1).[21] The ^{13}C{^{1}H} and ^{19}F{^{1}H} NMR spectra are also fully consistent with the formation of a low-symmetry heterodinuclear complex, and the separate signals for each of the two phenyl and benzyl carbons are particularly diagnostic (Figures S2−S6).[58]

The new catalyst was tested in CHO/CO_2 ROCOP, at 1 bar CO_2 pressure and in the presence of 4 equiv of CHD, and showed excellent activity and selectivity (TOF = 101 h^{-1}, 99% selective for carbonate linkages, Table S1, entry 1). It produced

https://dx.doi.org/10.1021/jacs.9b13106
J. Am. Chem. Soc. 2020, 142, 4367−4378

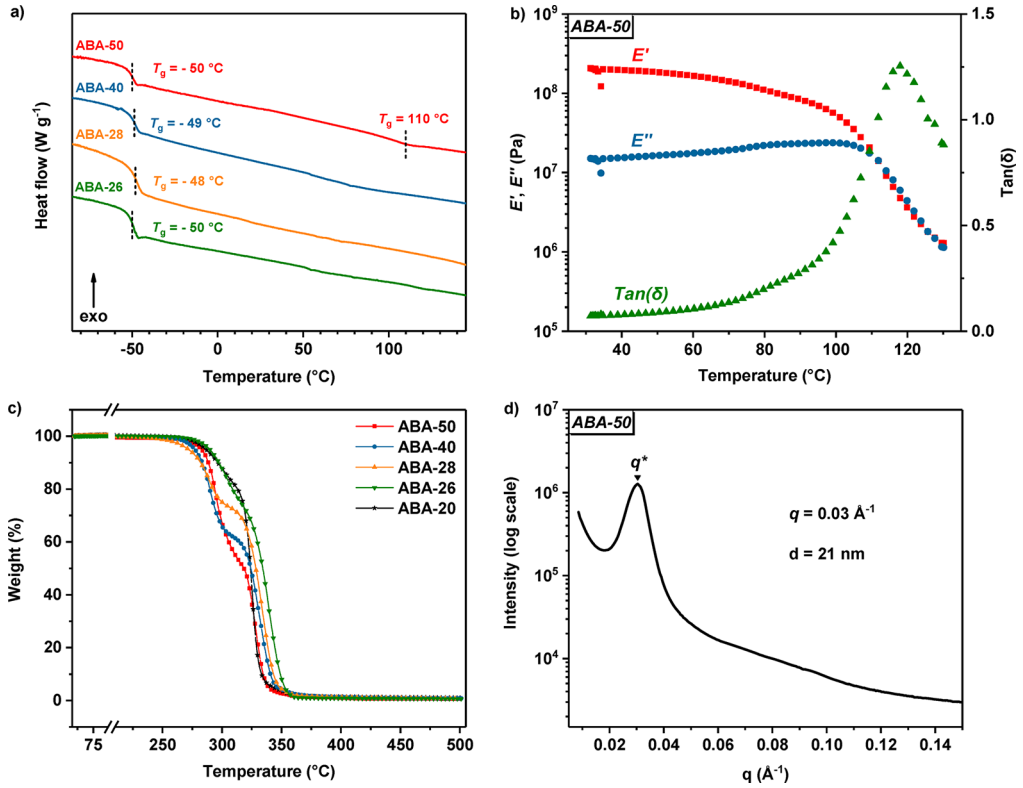

Figure 2. Characterization of ABA (PCHC-*b*-PDL-*b*-PCHC) triblock polymer series. (a) DSC thermograms: traces have been shifted vertically for clarity. (b) DMTA temperature sweep profile for sample ABA-50. Overlay of storage modulus (E'), loss modulus (E''), and tan(δ); conditions ω = 1 Hz, γ = 1%, heating rate 5 °C min^{-1} (Figures S19–S22 for DMTA of ABA-40 and ABA-26). (c) TGA profiles of ABA triblock polymers. Heating rate = 5 °C min^{-1} (Figures S23–S28 for the individual thermograms). (d) Small-angle X-ray scattering (SAXS) ABA-50 film at 25 °C with the principle scattering peak, q*, at 0.03 Å^{-1} (▼).

only dihydroxyl telechelic PCHC with a monomodal molar mass distribution and an overall M_n of 12.8 kg mol^{-1} (Table S1, Figure S7). It was also tested for ε-DL ROP, using identical conditions to previous runs and with only 4 equiv of CHD. It showed good activity, with a TOF of over 4500 h^{-1}, and yielded high molar mass PDL with a monomodal, narrow dispersity distribution (M_n = 33.1 kg mol^{-1}, $Đ$ = 1.10) (Table S1, Entry 2). The polymer chains were all α,ω-dihydroxyl telechelic as determined by MALDI-TOF mass spectrometry (Figure 1, bottom).

The new Zn(II)/Mg(II) organometallic catalyst was used to prepare a series of ABA triblock polymers using a one-pot procedure (Figure 1, Scheme 2). As a representative example, the preparation of ABA-50 is described. The reaction was conducted in two stages: first the catalyst was mixed with 600 equiv of DL and 700 of CHO resulting in efficient ε-DL ROP and the selective formation of dihydroxyl telechelic PDL. Near complete PDL formation (>90%) occurred within 20 min. Next, CO_2 was added at a pressure of 20 bar, and the polymerization stirred for a further 20 h until it reached >90% PCHC conversion. A sample of the crude material showed the formation of a high molar mass polymer (59.8 kg mol^{-1}, $Đ$ = 1.10) (Table 1, entry 5).

To better understand the monomer selectivity, a representative polymerization with the same wt % composition in the product (ABA-50), was performed in a Schlenk tube fitted with an in situ ATR-IR spectroscopic probe and using only 1 bar CO_2 pressure. Under these conditions there is less efficient reaction stirring, and so the overall reaction times are longer (rates are lower), but the catalytic selectivity is the same (Scheme 2).[21] The reaction shows an exponential growth of PDL, consistent with a first order dependence of rate on DL concentration. The polymerization kinetics are in line with previous investigations of lactone ROP.[59] Upon changing the gas atmosphere from nitrogen to carbon dioxide, the DL ROP stops and PCHC slowly begins to form (Scheme 2). The in situ analysis clearly shows the very high reaction selectivity: during the first reaction phase there is only formation of PDL, and once the CO_2 is added into the vessel, there is no further conversion of DL.

In terms of ABA-50 characterization data, the ^{1}H NMR spectrum shows quantitative selectivity for carbonate linkages (>99%) and for polymer formation (>99%) in the PCHC blocks. There are no signals corresponding to ether linkages or to cyclic carbonate (Figure S8). Moreover, since each monomer is >90% converted, the composition of the block polymer closely matches the starting monomer stoichiometry. The polymer composition remains the same after purification to remove excess epoxide (Figures S8–S9). The ^{13}C{^{1}H} NMR spectrum shows two different types of carbonyl signal, assigned to -ester and -carbonate blocks, respectively, and shows there is a lack of transesterification (Figure S10). Chain end-group analysis, by ^{31}P{^{1}H} NMR spectroscopy,[42] shows only PCHC hydroxyl end-groups and no remaining PDL end-groups (Figure S11). Together the data provide strong support for the ABA triblock structures.

The same switchable process was applied using a range of monomer compositions and producing a systematic series of different block polymers (Table 1 and Table S2). In all cases, the reactions were very well controlled with polymer

https://dx.doi.org/10.1021/jacs.9b13106
J. Am. Chem. Soc. 2020, 142, 4367–4378

Table 2. Mechanical Properties of ABA Triblock Polymers as a Function of Block Composition and Molar Mass

polymer	wt % PCHC	M_n (kg mol^{-1}) [$Đ$]	E_y[a] (MPa)	σ[b] (MPa)	ε_y[c] (%)	ε_b[d] (%)
ABA-50	50	59.8 [1.10]	238 ± 35	20 ± 2	9.0 ± 1.7	900 ± 104
ABA-40	40	49.4 [1.08]	81 ± 13	5.1 ± 0.2	17 ± 2	1920 ± 235
ABA-28	28	46.4 [1.07]	3.0 ± 0.8	0.85 ± 0.04	N.A.	1060 ± 54
ABA-26	26	71.9 [1.16]	3.9 ± 0.7	1.4 ± 0.1	N.A.	1400 ± 69

[a]Young's modulus. [b]Tensile strength. [c]Strain at yield point. [d]Strain at break. Mean values ± std. dev. from measurements conducted independently on at least 5 specimens.

composition being predictable from monomer stoichiometry. In all cases, monomer conversions were >90% and the overall molar mass was sufficiently high (45−60 kg mol^{-1}, DP = 300) to drive phase separation. The series comprises DL:CHO monomer ratios from 1:3.3 to 3:1, and delivers ABA polymers from 20 to 76 wt % PCHC (Table S2).

The reactions were all effective at low catalyst loadings (0.1−0.05 mol % vs monomers) and proceeded efficiently showing monomer conversions >90% within 20 h. A significant advantage of switchable catalysis is the removal of any intermediary or macroinitiator isolation and purification steps.

The series of polymers were all characterized using a range of spectroscopies and SEC to confirm their compositions and molar masses (Table 1). SEC analyses show minor amounts of lower molar mass PCHC (Figure S12). This forms during CO_2 addition when ppm quantities of water are also present as a contaminant in the gas stream. The residual water remains even after drying (using drying columns) and has already been shown to form diol (1,2-cyclohexane diol, CHD), which is a chain transfer agent.[56] In terms of the block polymer properties, minor residual PCHC is not considered deleterious particularly as the new triblocks are designed to optimize PCHC properties. The series of samples are labeled ABA-#, where the number refers to the weight percentage of PCHC (hard), which is determined from the composition data.

The series of polymers, from ABA-20 to ABA-76, were analyzed by thermogravimetric analysis (TGA) to assess thermal stability relevant for any future processing and application (Figures S23−S28). Onset degradation temperatures ($T_{d,5}$) were generally around 280 °C, which is consistent with purified PCHC.[60] The decomposition profiles differ according to the block polymer compositions and two step-profiles are observed (Figure 2c). For example, for ABA-50, the first degradation corresponds to 50% weight loss, consistent with the degradation of the PCHC. The second degradation, occurring at 322 °C, corresponds to 50% weight loss, consistent with PDL degradation. In all samples, the outer PCHC blocks are thermally degraded first, consistent with a chain-end scission process as the principal degradation. Overall, the $T_{d,5}$ value is at least 170 °C higher than the upper glass transition temperature for the PCHC blocks (T_g ∼110 °C), and this temperature range facilitates thermoplastic processing. Differential scanning calorimetry (DSC) shows the two blocks are amorphous and only glass transitions are observed (Figures S13−S18). For example, ABA-50 shows two T_g values at similar temperatures to the homopolymers ($T_{g,PDL}$ ≅ −58 °C,[61] $T_{g,PCHC}$ ≅ 110−120 °C[27,62]). Some of the other samples only show the lower T_g, by DSC analysis, although in all cases its value is close to −60 °C. According to the Fox−Flory relationship, block miscibility would give rise to $T_{g,mix}$ values from −23 to 7.5 °C, and thus, the blocks are likely to be phase separated.[63] The apparent absence of the upper T_g in the DSC thermograms of low PCHC content samples is likely caused by its reduced concentration and the low DSC signal intensity (Figures S13−S18).[64] Some of the samples were further investigated by dynamic mechanical thermal analysis (DMTA) to identify their upper T_g, and showed typical behaviors of viscoelastic materials (Figures 2b, S19−S22). The DMTA data for ABA-50 show that as the temperature increases from 30−100 °C, there is a gradual decrease in storage modulus E' (from 200 MPa) and an increase in loss modulus (E''). Correspondingly, the tan(δ), and glass transition temperature, is maximized at 118 °C. The T_g value for ABA-50 of 118 °C is consistent with the value obtained by DSC. DMTA also allows determination of the upper T_g (PCHC) for other samples and helps substantiate the phase separation (Figures S19−S22). Small-angle X-ray scattering (SAXS), applied to ABA-50, shows a strong principal scattering peak (with intensity q^*) corresponding to a domain spacing (d) of around 21 nm ($d = 2\pi/q^*$) (Figure 2d). The data are consistent with phase separation but suggest that there is only limited long-range order in the block polymer and, because higher order reflections are not observed, the exact block morphology could not be determined. Similar SAXS results were obtained for samples ABA-40 and ABA-26 (Figures S29−S30).

Mechanical Properties. ABA-50, -40, -28, -26 were successfully processed into films suitable for tensile mechanical experiments. Films of ∼150 μm were prepared via solvent casting from a methylene chloride solution (30 wt %) and were dried by solvent evaporation under ambient conditions for 72 h, and then in vacuo at 40 °C for a further 48 h. Dumbbell shaped samples were prepared, according to ISO 527−2 type 5B, and uniaxial extension experiments, conducted according to ISO 527, were used to derive stress vs strain relationships (10 mm min^{-1} cross-head speed). The mechanical properties of the triblock polymers vary as a function of the relative PCHC (hard-block) weight fraction (Table 2). The tensile stress−strain curves show that samples ABA-50 and ABA-40 have behaviors typical of ductile plastics with yield points at ∼9% and ∼17% strain, respectively (Figure 3 red and blue curves). Beyond the yield points, both materials exhibit plastic deformation and undergo significant strain-hardening (Figure S31(a)). ABA-50 shows the highest tensile strength (20 MPa), and a very high elongation at break (900%). It shows a tensile toughness (U_T), estimated from the stress−strain data, of 112 MJ m^{-3}.

ABA-28 exhibits elastomeric behavior and does not show any obvious yield point. Accordingly, the samples of ABA-28 quickly recover their original shapes once stress is released and show no permanent plastic deformation even beyond the point of fracture (Figures 3, orange curve, and S31(b)). ABA-28 shows high elasticity, with high values of elongation at break (>1000%) and a low ultimate tensile strength. To explore further, ABA-26 was synthesized with a similar composition to ABA-28 but with higher molar mass (M_n = 70 kg mol^{-1}).

https://dx.doi.org/10.1021/jacs.9b13106
J. Am. Chem. Soc. 2020, 142, 4367−4378

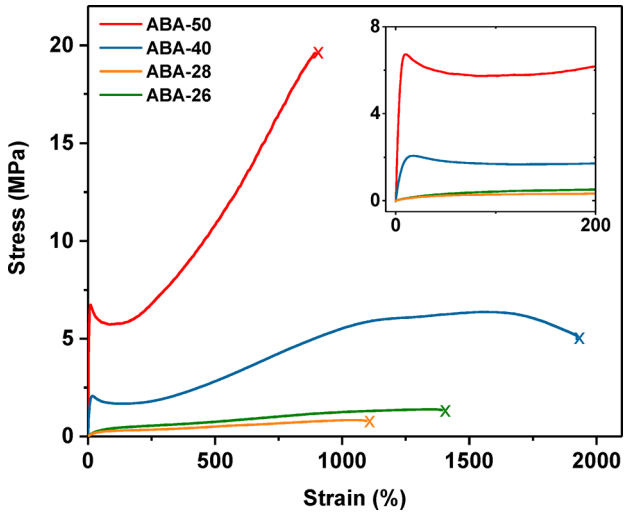

Figure 3. Stress−strain curves for uniaxial extension measurements of ABA triblock polymers. Failure points marked with an "X". Inset: enlargement of the 0−200% strain region.

Increasing the overall polymer molar mass significantly increases the elongation at break but only slightly changes the ultimate tensile strength. Such high elasticity, low tensile strength materials are of future interest as mimics of elastin and other soft natural materials.[65] The two elastomers, ABA-26 and ABA-28, were subjected to ten repeated stress−strain cycles, where samples were stretched to 200% elongation, the stress removed and the sample relaxed at 10 mm min^{-1}, and then the stress repeated (Figures S32−S33). Both materials showed a slight reduction in Young's modulus and stress between the first and second cycles, which indicates slight plastic deformation in the first cycle. Thereafter both materials show high elastic recovery values, specifically these were 75% for ABA-26 and 95% for ABA-28.

The two plastics, ABA-40 and ABA-50, showed strain-induced plastic-to-rubber transitions (Figures S34−S35). In hysteresis experiments (0−200% strain, 10 cycles), a clear yield point was observed in the first cycles, yet subsequent cycles showed elastic profiles. It is hypothesized that the plastic-to-rubber transition is due to a change in the polymer microstructure so that there is isolation and alignment of PCHC domains within the PDL matrix.[46] Similar behavior has previously been observed for poly(styrene-butadiene-styrene) (SBS) materials and for block polyesters.[66−68]

The remaining samples containing high quantities of PCHC or PDL, respectively, and pure PDL could not be processed into freestanding films. For example, ABA-20 is highly viscoelastic and cannot retain its shape on removal from the mold (Figure S36(a)). In contrast, ABA-76 is very brittle, and shatters under minimal stress (Figure S36(b)). Attempts to analyze a 50:50 wt % mixture of PCHC and PDL showed macrophase separation with the brittle PCHC layer being suspended above the softer PDL layer. The polymer blends could not be processed or analyzed further and would clearly be very difficult to practically apply (Figure S36(c)). One future application for these block polymers could be as blend compatibilization.

Samples of ABA-20 were assessed as pressure sensitive adhesives. Oscillatory rheology was used to probe its viscoelastic properties. A frequency sweep reveals the regions over which the viscous (G'') and elastic (G') components dominate (Figure 4a). The shear storage modulus, G', and shear loss modulus, G'', at frequencies consistent with adhesive bonding (10^{-1} rad s^{-1}) and debonding (10^{2} rad s^{-1}), were used to construct a viscoelastic window. The data suggest ABA-20 could be used as a high shear, permanent adhesive (Figure 4b).[69] The bonding aspect of the window (lower boundary) lies below the Dahlquist criterion ($G' \leq 3 \times 10^5$ Pa), indicating ABA-20 should be a contact efficient or pressure-sensitive adhesive (PSA) without needing further additives.[69,70] A fixed oscillation vs time experiment showed a stable storage modulus (G'), at 2.6×10^5 Pa, and at a value which is consistently higher than the loss modulus (G''); i.e., ABA-20 is a soft, viscoelastic solid (Figure S37). The adhesive properties of ABA-20 were assessed using 180° peel, and loop-tack tests, using pressure-sensitive tape council (PSTC) grade polished stainless steel as the substrate and 5 μm thick PETE film (Mylar) as the adhesive backing. The samples were coated onto the PETE sheet, from a 30 wt % solution in DCM using a wound wire rod, and the film thickness was ~60 μm. ABA-20 displays a maximum peel force ~10 N cm^{-1} (Figure S38). The loop tack test shows an average maximum tack force ~8.7 N cm^{-1} (Figure S39). A cross-hatch test, with ABA-20 coated onto PSTC-grade stainless steel, showed only minimal coating removal on application and removal of scotch tape (ISO classification: 1). These data are indicative of strong adhesive bonding to steel (Figure S40).

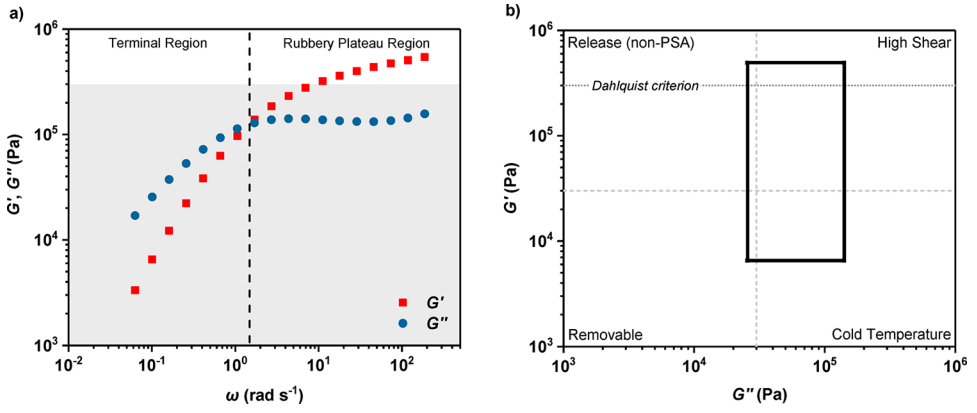

Figure 4. (a) Frequency sweep of ABA-20. Gray shaded area represents the Dahlquist criterion ($G' \leq 3 \times 10^5$ Pa). (b) Viscoelastic window for ABA-20 constructed from the bonding (ω = 0.1 rad s^{-1}) and debonding (ω = 100 rad s^{-1}) frequencies. Quadrant titles indicate PSA type.

https://dx.doi.org/10.1021/jacs.9b13106
J. Am. Chem. Soc. 2020, 142, 4367−4378

DISCUSSION

The ABA triblock polymers, PCHC-*b*-PDL-*b*-PCHC, are prepared with straightforward and efficient catalysis. Lactone ring-opening polymerization delivers the central PDL soft-block, and by simply adding carbon dioxide into the reaction vessel, two outer PCHC hard-blocks are attached. The new catalyst increases reaction rates, maximizes polymer molar masses, and controls its structure. It is applied at low loadings, from 1:1000−1:2000 (catalyst: CHO + DL) and in toluene solutions (3 M); it is highly active with turnover frequency (TOF) values for DL ROP exceeding 4000 h^{-1} and for CHO/CO_2 ROCOP of 100 h^{-1}. The high performance allows reactions to be conducted using minimized catalyst residues (0.1−0.05 mol %), at acceptable reactor residence times (<24 h) and with monomer conversions >90% obviating monomer removal strategies at the end of reaction. The catalytic activity is up to 20 times higher than previously reported CO_2/CHO ROCOP (TOF = 5 h^{-1} under comparable conditions) and 90 times higher than previously reported lactone ROP (TOF = 50 h^{-1} for ε-caprolactone ROP under comparable conditions).[37,40] The catalysis is also well-controlled and delivers predictable block compositions and structures. By applying the new process, ABA block polymers with variable PCHC weight ratios and carbon dioxide uptakes are easily produced.

By controlling the CO_2 utilization and position in the polymer chain, the properties vary from viscoelastic pressure sensitive adhesives (ABA-20), to high elongation thermoplastic elastomers (ABA-26 and ABA-28) to, at highest CO_2 utilization, toughened plastics (ABA-40 and ABA-50). There is clearly a much broader scope of applications for PCHC than was previously envisaged. Considering specifically adhesives applications ABA-20, with a ∼6 wt % CO_2 content, shows good performance as a single-component pressure-sensitive adhesive. It has a low dynamic elastic modulus, below the Dahlquist criterion for adhesives, and, in contact with steel surfaces, shows both high peel (10 N cm^{-1}) and tack strengths (8.7 N cm^{-1}). It has higher peel strength than commercial adhesives such as duct, masking, electrical, and scotch tape, and these commercial adhesives are formulated products, comprising mixtures of polymers, plasticizers, fillers, and tackifiers. In contrast, the data for ABA-20 are stand-alone, but future investigations should also apply these CO_2-derived polymers in formulations.[71]

The promising characteristics of ABA-20 suggest it could be used instead of styrenic, polyacrylate, or natural rubber, currently applied as the polymeric component in adhesives. ABA-20 also shows equivalent, or better, performance than leading triblock polymer pressure-sensitive adhesives, applied with tackifiers, which were reported in the literature.[72−76] It is compared to biobased block polyester and polyacrylate based adhesives, which were applied with various tackifiers, some biobased (see Figure S41 for illustrations of their structures).[72−76] In particular, it is bench-marked against ABA block polyesters, comprising polylactide A-blocks and soft B-blocks derived from menthide or ε-decalactone (Figures 5, S41).[72,74,75,77−79] ABA-20 shows higher peel force strength than the corresponding bioderived ABA polyester or acrylate polymer/tackifier blends and illustrates the benefits of PCHC rigid blocks.[71−73,75] Further, higher operating temperatures are anticipated since PCHC (T_g = 110−120 °C) has a considerably higher glass transition temperature than PLA (T_g = 50−60 °C). Compared to the highest performing

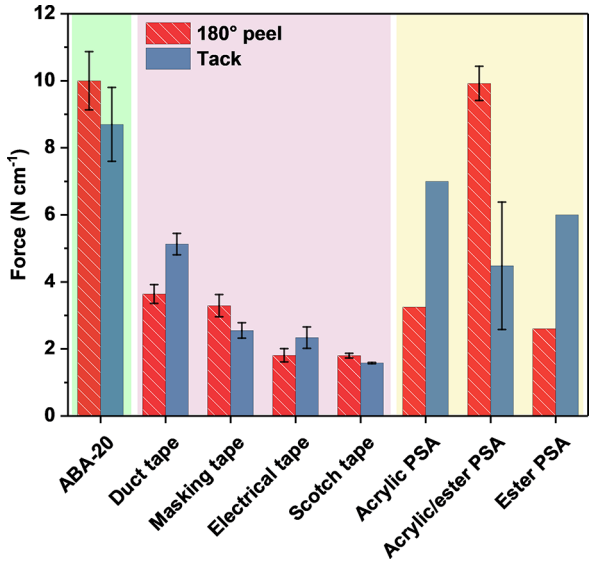

Figure 5. Adhesive performance, in peel and tack testing modes, for triblock ABA-20 (green highlight) and selected commercial (purple highlight) and literature (yellow highlight) PSAs. Acrylic PSA = PAAI-PEHA-PAAI;[73] acrylic/ester PSA = PMeMBL-PM-PMeMBL;[72] ester PSA = PLLA-PDL-PLLA[71] (see Figure S41 for polymer structures).

polyacrylate pressure-sensitive adhesives, particularly those mimicking muscle adhesion, the peel force and tack results are modest,[80,81] demonstrating the significant scope to optimize structures in the future.[82]

Increasing the CO_2 content to ∼15 wt % in sample ABA-50 yields a toughened plastic. ABA-50 shows significantly higher toughness, through the incorporation of the soft PDL midblock, than PCHC alone and overcomes the well-known brittleness of PCHC (Figure 6). Compared with bioderived poly(limonene carbonate) (PLimC), prepared by ROCOP of limonene oxide/CO_2, ABA-50 shows significantly higher tensile toughness (U_T): ∼3.15 MJ m^{-3} for PLimC,[83] compared to 112 MJ m^{-3} for ABA-50. One future application signaled by these results is as a compatibilizer and impact modifier for well-known PCHC or PLimC. A very recent report of PBL-*b*-PCHC showed at 50 wt % PCHC incorporation a similar tensile strength of 17 MPa but with just 1.3% elongation at break.[51] In terms of benchmarking the performance of ABA-50 against other plastics, it shows higher toughness, but considerably lower tensile strength, than the well-known commercial polycarbonate, prepared from bisphenol A (U_T ∼ 19 MJ m^{-3}) (Figure S42). It also significantly improves upon the toughness of popular biobased plastic polylactide (PLA), with toughened PLA showing U_T ∼ 18 MJ m^{-3}, and maintains comparable ultimate tensile strength to toughened PLA (25.8 MPa).[84,85]

Given the encouraging properties of ABA-50 and the straightforward method to prepare it, future research could focus on how to exploit its high toughness and increase tensile strength. For example, using isotactic PCHC blocks to enhance rigidity or incorporation of vinyl-cyclohexene oxide as a cross-linkable group in the carbonate block could both offer means to increase tensile strength.[36,86] An additional advantage of using commercially available vinyl-substituted epoxides is the facility to "pattern" the resulting materials and install functionalities that control hydrophilicity, filler binding, and/or pH responsiveness.[87] Another feature of these triblock

https://dx.doi.org/10.1021/jacs.9b13106
J. Am. Chem. Soc. 2020, 142, 4367−4378

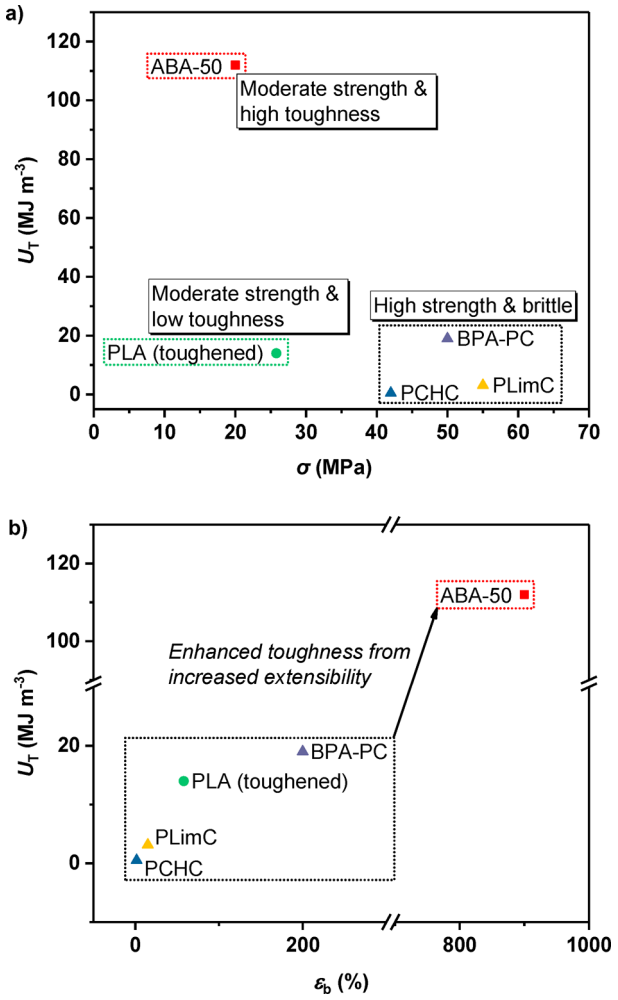

Figure 6. Ashby plots of tensile toughness (U_T) vs (a) tensile strength (σ) and (b) elongation at break (ε_b) for comparison of ABA-50 with selected commercial and literature materials. Materials classified as polycarbonate (▲), polyester (●), or poly(carbonate-*b*-ester-*b*-carbonate) (■).

polymers is that they contain a high proportion of bioderived raw material and are easily prepared from commercially available monomers. Considering that ε-decalactone is biosourced from castor oil via ricinoleic acid,[88,89] and that the CO_2 content is straightforward to control, the polymers offer theoretical renewable contents from 47% (ABA-76) to 86% (ABA-20). Currently, cyclohexene oxide is produced from petrochemicals, but routes from triglyceride coproducts could be adopted in the future if fully biobased content were required.[90]

In terms of end-of-life scenarios, the ester and carbonate linkages comprising the polymer backbone are expected to ultimately render the materials degradable. Moreover, degradation products, in the form of diols, hydroxy-acids, and CO_2, are not anticipated to be toxic. Preliminary stability studies showed that films of ABA-50 are stable to mass loss in acidic and basic media at ambient temperature for at least a period of 9 months.

Nonetheless, the samples could be fully degraded by dissolving them in toluene, warming to 60 °C (to accelerate the rate of degradation), and treatment with a weak acid ([*p*-toluene sulfonic acid] = 5 mM). Under these conditions rapid loss of polymer molar mass occurred over a period of 96 h (Figure S43).

CONCLUSIONS

A switchable polymer synthesis protocol, using a new heterodinuclear Zn(II)/Mg(II) organometallic catalyst, allows for the fast, efficient, and controllable preparation of fully degradable ABA block polymers. The protocol is applied to prepare a logical series of ABA type poly(cyclohexene carbonate)-*b*-poly(ε-decalactone)-*b*-poly(cyclohexene carbonate), with 6−31 wt % of the material derived from CO_2. The polymers show promising thermal and mechanical properties, and progressively greater CO_2 utilization allows control over applications spanning viscoelastic adhesives, thermoplastic elastomers, and tough plastics. These block polymers overcome the well-known brittleness of PCHC, one of the most widely studied CO_2-derived polymers. Further, a range of new properties for CO_2-containing polymers are demonstrated, which expands their application scope well-beyond polyols for polyurethane. Viewed from the perspective of aliphatic polyesters, the cyclohexylene carbonate units confer reinforcement, mechanical strength, and increased service temperature to the resulting copolymers and provide a viable and, in some cases, better performing alternative "hard" block to PLA. The range of future polymers and applications enabled by the polymerization process could indeed be very large, since it is expected to be generally applicable to a wide range of lactones, lactide, epoxides, anhydrides, and heterocumulenes.

ASSOCIATED CONTENT

Supporting Information

The Supporting Information is available free of charge at https://pubs.acs.org/doi/10.1021/jacs.9b13106.

Detailed experimental procedures for catalyst synthesis and polymerizations, and catalyst and polymer characterization data (1D and 2D NMR, SEC, DSC, DMTA, TGA, SAXS) (PDF)

AUTHOR INFORMATION

Corresponding Author

Charlotte K. Williams − *Department of Chemistry, Chemistry Research Laboratory, University of Oxford, Oxford OX1 3TA, U.K.*; orcid.org/0000-0002-0734-1575; Email: charlotte.williams@chem.ox.ac.uk

Authors

Gregory S. Sulley − *Department of Chemistry, Chemistry Research Laboratory, University of Oxford, Oxford OX1 3TA, U.K.*

Georgina L. Gregory − *Department of Chemistry, Chemistry Research Laboratory, University of Oxford, Oxford OX1 3TA, U.K.*

Thomas T. D. Chen − *Department of Chemistry, Chemistry Research Laboratory, University of Oxford, Oxford OX1 3TA, U.K.*

Leticia Peña Carrodeguas − *Department of Chemistry, Chemistry Research Laboratory, University of Oxford, Oxford OX1 3TA, U.K.*

Gemma Trott − *Department of Chemistry, Chemistry Research Laboratory, University of Oxford, Oxford OX1 3TA, U.K.*

https://dx.doi.org/10.1021/jacs.9b13106
J. Am. Chem. Soc. 2020, 142, 4367−4378

Alba Santmarti − *Department of Aeronautics, Imperial College London, London SW7 2AZ, U.K.*

Koon-Yang Lee − *Department of Aeronautics, Imperial College London, London SW7 2AZ, U.K.;* orcid.org/0000-0003-0777-2292

Nicholas J. Terrill − *Beamline I22, Diamond Light Source, Harwell Science and Innovation Campus, Didcot OX11 0DE, U.K.*

Complete contact information is available at: https://pubs.acs.org/10.1021/jacs.9b13106

Notes

The authors declare the following competing financial interest(s): C.K.W is a director of Econic Technologies Ltd.

■ ACKNOWLEDGMENTS

Professor Clive Siviour and his research team, Department of Materials, University of Oxford are sincerely thanked for allowing access to DMTA and for rheology measurements. We acknowledge the I22 team at Diamond Light Source for support during SAXS measurements and beam-time allocation under proposal SM23087-1. The EPSRC (EP/S018603/1, EP/L017393/1, EP/K014668/1) and DTG (TC, GS) are acknowledged for research funding.

■ REFERENCES

(1) Kamphuis, A. J.; Picchioni, F.; Pescarmona, P. P. CO2-fixation into cyclic and polymeric carbonates: principles and applications. *Green Chem.* **2019**, *21* (3), 406−448.

(2) Artz, J.; Müller, T. E.; Thenert, K.; Kleinekorte, J.; Meys, R.; Sternberg, A.; Bardow, A.; Leitner, W. Sustainable Conversion of Carbon Dioxide: An Integrated Review of Catalysis and Life Cycle Assessment. *Chem. Rev.* **2018**, *118* (2), 434−504.

(3) Burkart, M. D.; Hazari, N.; Tway, C. L.; Zeitler, E. L. Opportunities and Challenges for Catalysis in Carbon Dioxide Utilization. *ACS Catal.* **2019**, *9* (9), 7937−7956.

(4) Hepburn, C.; Adlen, E.; Beddington, J.; Carter, E. A.; Fuss, S.; Mac Dowell, N.; Minx, J. C.; Smith, P.; Williams, C. K. The technological and economic prospects for CO2 utilization and removal. *Nature* **2019**, *575* (7781), 87−97.

(5) Longo, J. M.; Sanford, M. J.; Coates, G. W. Ring-Opening Copolymerization of Epoxides and Cyclic Anhydrides with Discrete Metal Complexes: Structure−Property Relationships. *Chem. Rev.* **2016**, *116* (24), 15167−15197.

(6) Zhu, Y.; Romain, C.; Williams, C. K. Sustainable Polymers from Renewable Resources. *Nature* **2016**, *540* (7633), 354−362.

(7) Darensbourg, D. J. Chain transfer agents utilized in epoxide and CO2 copolymerization processes. *Green Chem.* **2019**, *21* (9), 2214−2223.

(8) Langanke, J.; Wolf, A.; Hofmann, J.; Bohm, K.; Subhani, M. A.; Muller, T. E.; Leitner, W.; Gurtler, C. Carbon dioxide (CO2) as sustainable feedstock for polyurethane production. *Green Chem.* **2014**, *16* (4), 1865−1870.

(9) Scharfenberg, M.; Hilf, J.; Frey, H. Functional Polycarbonates from Carbon Dioxide and Tailored Epoxide Monomers: Degradable Materials and Their Application Potential. *Adv. Funct. Mater.* **2018**, *28* (10), 16.

(10) Stosser, T.; Li, C. L.; Unruangsri, J.; Saini, P. K.; Sablong, R. J.; Meier, M. A. R.; Williams, C. K.; Koning, C. Bio-derived polymers for coating applications: comparing poly(limonene carbonate) and poly (cyclohexadiene carbonate). *Polym. Chem.* **2017**, *8* (39), 6099−6105.

(11) Alagi, P.; Ghorpade, R.; Choi, Y. J.; Patil, U.; Kim, I.; Baik, J. H.; Hong, S. C. Carbon Dioxide-Based Polyols as Sustainable Feedstock of Thermoplastic Polyurethane for Corrosion-Resistant Metal Coating. *ACS Sustainable Chem. Eng.* **2017**, *5* (5), 3871−3881.

(12) Hauenstein, O.; Agarwal, S.; Greiner, A. Bio-based polycarbonate as synthetic toolbox. *Nat. Commun.* **2016**, *7*, 11862.

(13) DeBolt, M.; Kiziltas, A.; Mielewski, D.; Waddington, S.; Nagridge, M. J. Flexible polyurethane foams formulated with polyols derived from waste carbon dioxide. *J. Appl. Polym. Sci.* **2016**, *133* (45), 9.

(14) Lee, S. H.; Cyriac, A.; Jeon, J. Y.; Lee, B. Y. Preparation of thermoplastic polyurethanes using in situ generated poly(propylene carbonate)-diols. *Polym. Chem.* **2012**, *3* (5), 1215−1220.

(15) von der Assen, N.; Bardow, A. Life cycle assessment of polyols for polyurethane production using CO2 as feedstock: insights from an industrial case study. *Green Chem.* **2014**, *16* (6), 3272−3280.

(16) Chapman, A. M.; Keyworth, C.; Kember, M. R.; Lennox, A. J. J.; Williams, C. K. Adding Value to Power Station Captured CO2: Tolerant Zn and Mg Homogeneous Catalysts for Polycarbonate Polyol Production. *ACS Catal.* **2015**, *5* (3), 1581−1588.

(17) Wang, Y. Y.; Darensbourg, D. J. Carbon dioxide-based functional polycarbonates: Metal catalyzed copolymerization of CO2 and epoxides. *Coord. Chem. Rev.* **2018**, *372*, 85−100.

(18) Kozak, C. M.; Ambrose, K.; Anderson, T. S. Copolymerization of carbon dioxide and epoxides by metal coordination complexes. *Coord. Chem. Rev.* **2018**, *376*, 565−587.

(19) Paul, S.; Zhu, Y. Q.; Romain, C.; Brooks, R.; Saini, P. K.; Williams, C. K. Ring-opening copolymerization (ROCOP): synthesis and properties of polyesters and polycarbonates. *Chem. Commun.* **2015**, *51* (30), 6459−6479.

(20) Kissling, S.; Lehenmeier, M. W.; Altenbuchner, P. T.; Kronast, A.; Reiter, M.; Deglmann, P.; Seemann, U. B.; Rieger, B. Dinuclear zinc catalysts with unprecedented activities for the copolymerization of cyclohexene oxide and CO2. *Chem. Commun.* **2015**, *51* (22), 4579−4582.

(21) Trott, G.; Garden, J. A.; Williams, C. K. Heterodinuclear Zinc and Magnesium Catalysts for Epoxide/CO_2 Ring Opening Copolymerizations. *Chem. Sci.* **2019**, *10* (17), 4618−4627.

(22) Kember, M. R.; Williams, C. K. Efficient Magnesium Catalysts for the Copolymerization of Epoxides and CO2; Using Water to Synthesize Polycarbonate Polyols. *J. Am. Chem. Soc.* **2012**, *134* (38), 15676−15679.

(23) Buchard, A.; Jutz, F.; Kember, M. R.; White, A. J. P.; Rzepa, H. S.; Williams, C. K. Experimental and Computational Investigation of the Mechanism of Carbon Dioxide/Cyclohexene Oxide Copolymerization Using a Dizinc Catalyst. *Macromolecules* **2012**, *45* (17), 6781−6795.

(24) Jutz, F.; Buchard, A.; Kember, M. R.; Fredriksen, S. B.; Williams, C. K. Mechanistic Investigation and Reaction Kinetics of the Low-Pressure Copolymerization of Cyclohexene Oxide and Carbon Dioxide Catalyzed by a Dizinc Complex. *J. Am. Chem. Soc.* **2011**, *133* (43), 17395−17405.

(25) Saini, P. K.; Romain, C.; Williams, C. K. Dinuclear metal catalysts: improved performance of heterodinuclear mixed catalysts for CO_2-epoxide copolymerization. *Chem. Commun.* **2014**, *50* (32), 4164−4167.

(26) Thorat, S. D.; Phillips, P. J.; Semenov, V.; Gakh, A. Physical properties of aliphatic polycarbonates made from CO2 and epoxides. *J. Appl. Polym. Sci.* **2003**, *89* (5), 1163−1176.

(27) Koning, C.; Wildeson, J.; Parton, R.; Plum, B.; Steeman, P.; Darensbourg, D. J. Synthesis and physical characterization of poly(cyclohexane carbonate), synthesized from CO2 and cyclohexene oxide. *Polymer* **2001**, *42* (9), 3995−4004.

(28) Li, G. F.; Qin, Y. S.; Wang, X. H.; Zhao, X. J.; Wang, F. S. Study on the influence of metal residue on thermal degradation of poly(cyclohexene carbonate). *J. Polym. Res.* **2011**, *18* (5), 1177−1183.

(29) Zhao, Y. J.; Wang, Y.; Zhou, X. P.; Xue, Z. G.; Wang, X. H.; Xie, X. L.; Poli, R. Oxygen-Triggered Switchable Polymerization for the One-Pot Synthesis of CO2-Based Block Copolymers from Monomer Mixtures. *Angew. Chem., Int. Ed.* **2019**, *58* (40), 14311−14318.

(30) Zhang, Y.-Y.; Yang, G.-W.; Wu, G.-P. A Bifunctional β-Diiminate Zinc Catalyst with CO2/Epoxides Copolymerization and

RAFT Polymerization Capacities for Versatile Block Copolymers Construction. *Macromolecules* **2018**, *51* (10), 3640−3646.
(31) Wang, Y.; Zhao, Y. J.; Ye, Y. S.; Peng, H. Y.; Zhou, X. P.; Xie, X. L.; Wang, X. H.; Wang, F. S. A One-Step Route to CO2-Based Block Copolymers by Simultaneous ROCOP of CO2/Epoxides and RAFT Polymerization of Vinyl Monomers. *Angew. Chem., Int. Ed.* **2018**, *57* (14), 3593−3597.
(32) Reiter, M.; Kronast, A.; Kissling, S.; Rieger, B. In Situ Generated ABA Block Copolymers from CO2, Cyclohexene Oxide, and Poly(dimethylsiloxane)s. *ACS Macro Lett.* **2016**, *5* (3), 419−423.
(33) Cyriac, A.; Lee, S. H.; Varghese, J. K.; Park, E. S.; Park, J. H.; Lee, B. Y. Immortal CO2/Propylene Oxide Copolymerization: Precise Control of Molecular Weight and Architecture of Various Block Copolymers. *Macromolecules* **2010**, *43* (18), 7398−7401.
(34) Darensbourg, D. J.; Wu, G. P. A One-Pot Synthesis of a Triblock Copolymer from Propylene Oxide/Carbon Dioxide and Lactide: Intermediacy of Polyol Initiators. *Angew. Chem., Int. Ed.* **2013**, *52* (40), 10602−10606.
(35) Kember, M. R.; Copley, J.; Buchard, A.; Williams, C. K. Triblock copolymers from lactide and telechelic poly(cyclohexene carbonate). *Polym. Chem.* **2012**, *3* (5), 1196−1201.
(36) Kim, J. G.; Cowman, C. D.; LaPointe, A. M.; Wiesner, U.; Coates, G. W. Tailored Living Block Copolymerization: Multiblock Poly(cyclohexene carbonate)s with Sequence Control. *Macromolecules* **2011**, *44* (5), 1110−1113.
(37) Romain, C.; Williams, C. K. Chemoselective Polymerization Control: From Mixed-Monomer Feedstock to Copolymers. *Angew. Chem., Int. Ed.* **2014**, *53* (6), 1607−1610.
(38) Chen, T. T. D.; Zhu, Y.; Williams, C. K. Pentablock Copolymer from Tetracomponent Monomer Mixture Using a Switchable Dizinc Catalyst. *Macromolecules* **2018**, *51* (14), 5346−5351.
(39) Kernbichl, S.; Reiter, M.; Adams, F.; Vagin, S.; Rieger, B. CO2-Controlled One-Pot Synthesis of AB, ABA Block, and Statistical Terpolymers from beta-Butyrolactone, Epoxides, and CO2. *J. Am. Chem. Soc.* **2017**, *139* (20), 6787−6790.
(40) Paul, S.; Romain, C.; Shaw, J.; Williams, C. K. Sequence Selective Polymerization Catalysis: A New Route to ABA Block Copoly(ester-b-carbonate-b-ester). *Macromolecules* **2015**, *48* (17), 6047−6056.
(41) Li, X.; Hu, C.; Pang, X.; Duan, R.; Chen, X. One-pot copolymerization of epoxides/carbon dioxide and lactide using a ternary catalyst system. *Catal. Sci. Technol.* **2018**, *8* (24), 6452−6457.
(42) Stößer, T.; Chen, T. T. D.; Zhu, Y.; Williams, C. K. 'Switch' Catalysis: From Monomer Mixtures to Sequence-Controlled Block Copolymers. *Philos. Trans. R. Soc., A* **2018**, *376* (2110), 20170066.
(43) Romain, C.; Zhu, Y.; Dingwall, P.; Paul, S.; Rzepa, H. S.; Buchard, A.; Williams, C. K. Chemoselective Polymerizations from Mixtures of Epoxide, Lactone, Anhydride, and Carbon Dioxide. *J. Am. Chem. Soc.* **2016**, *138* (12), 4120−4131.
(44) Stößer, T.; Sulley, G. S.; Gregory, G. L.; Williams, C. K. Easy Access to Oxygenated Block Polymers via Switchable Catalysis. *Nat. Commun.* **2019**, *10* (1), 2668−2677.
(45) Raman, S. K.; Raja, R.; Arnold, P. L.; Davidson, M. G.; Williams, C. K. Waste Not, Want Not: CO_2 (Re)Cycling into Block Polymers. *Chem. Commun.* **2019**, *55* (51), 7315−7318.
(46) Zhu, Y.; Radlauer, M. R.; Schneiderman, D. K.; Shaffer, M. S. P.; Hillmyer, M. A.; Williams, C. K. Multiblock Polyesters Demonstrating High Elasticity and Shape Memory Effects. *Macromolecules* **2018**, *51* (7), 2466−2475.
(47) Stößer, T.; Williams, C. K. Selective Polymerization Catalysis from Monomer Mixtures: Using a Commercial Cr-Salen Catalyst To Access ABA Block Polyesters. *Angew. Chem., Int. Ed.* **2018**, *57* (21), 6337−6341.
(48) Stößer, T.; Mulryan, D.; Williams, C. K. Switch Catalysis To Deliver Multi-Block Polyesters from Mixtures of Propene Oxide, Lactide, and Phthalic Anhydride. *Angew. Chem., Int. Ed.* **2018**, *57* (51), 16893−16897.
(49) Zhu, Y.; Romain, C.; Williams, C. K. Selective polymerization catalysis: controlling the metal chain end group to prepare block copolyesters. *J. Am. Chem. Soc.* **2015**, *137* (38), 12179−12182.
(50) Ji, H.-Y.; Wang, B.; Pan, L.; Li, Y.-S. One-Step Access to Sequence-Controlled Block Copolymers by Self-Switchable Organocatalytic Multicomponent Polymerization. *Angew. Chem., Int. Ed.* **2018**, *57* (51), 16888−16892.
(51) Kernbichl, S.; Reiter, M.; Mock, J.; Rieger, B. Terpolymerization of β-Butyrolactone, Epoxides, and CO2: Chemoselective CO2-Switch and Its Impact on Kinetics and Material Properties. *Macromolecules* **2019**, *52* (21), 8476−8483.
(52) Winkler, M.; Romain, C.; Meier, M. A. R.; Williams, C. K. Renewable Polycarbonates and Polyesters from 1,4-Cyclohexadiene. *Green Chem.* **2015**, *17* (1), 300−306.
(53) Nagae, H.; Aoki, R.; Akutagawa, S.-n.; Kleemann, J.; Tagawa, R.; Schindler, T.; Choi, G.; Spaniol, T. P.; Tsurugi, H.; Okuda, J.; Mashima, K. Lanthanide Complexes Supported by a Trizinc Crown Ether as Catalysts for Alternating Copolymerization of Epoxide and CO2: Telomerization Controlled by Carboxylate Anions. *Angew. Chem., Int. Ed.* **2018**, *57* (9), 2492−2496.
(54) Deacy, A. C.; Durr, C. B.; Garden, J. A.; White, A. J. P.; Williams, C. K. Groups 1, 2 and Zn(II) Heterodinuclear Catalysts for Epoxide/CO2 Ring-Opening Copolymerization. *Inorg. Chem.* **2018**, *57* (24), 15575−15583.
(55) Romain, C.; Garden, J. A.; Trott, G.; Buchard, A.; White, A. J. P.; Williams, C. K. Di-Zinc-Aryl Complexes: CO2 Insertions and Applications in Polymerisation Catalysis. *Chem. - Eur. J.* **2017**, *23*, 7367−7376.
(56) Wu, G.-P.; Darensbourg, D. J. Mechanistic Insights into Water-Mediated Tandem Catalysis of Metal-Coordination CO_2/Epoxide Copolymerization and Organocatalytic Ring-Opening Polymerization: One-Pot, Two Steps, and Three Catalysis Cycles for Triblock Copolymers Synthesis. *Macromolecules* **2016**, *49* (3), 807−814.
(57) Romain, C.; Garden, J. A.; Trott, G.; Buchard, A.; White, A. J. P.; Williams, C. K. Di-Zinc−Aryl Complexes: CO2 Insertions and Applications in Polymerisation Catalysis. *Chem. - Eur. J.* **2017**, *23* (30), 7367−7376.
(58) Deacy, A. C.; Durr, C. B.; Garden, J. A.; White, A. J. P.; Williams, C. K. Groups 1, 2 and Zn(II) Heterodinuclear Catalysts for Epoxide/CO2 Ring-Opening Copolymerization. *Inorg. Chem.* **2018**, *57* (24), 15575−15583.
(59) van der Meulen, I.; Gubbels, E.; Huijser, S.; Sablong, R.; Koning, C. E.; Heise, A.; Duchateau, R. Catalytic Ring-Opening Polymerization of Renewable Macrolactones to High Molecular Weight Polyethylene-like Polymers. *Macromolecules* **2011**, *44* (11), 4301−4305.
(60) Radlauer, M. R.; Sinturel, C.; Asai, Y.; Arora, A.; Bates, F. S.; Dorfman, K. D.; Hillmyer, M. A. Morphological Consequences of Frustration in ABC Triblock Polymers. *Macromolecules* **2017**, *50* (1), 446−458.
(61) Lin, J.-O.; Chen, W.; Shen, Z.; Ling, J. Homo- and Block Copolymerizations of ε-Decalactone with l-Lactide Catalyzed by Lanthanum Compounds. *Macromolecules* **2013**, *46* (19), 7769−7776.
(62) Zhou, Y.; Duan, R.; Li, X.; Pang, X.; Wang, X.; Chen, X. Preparation and Thermal Properties of Polycarbonates/esters Catalyzed by Using Dinuclear Salph-Al from Ring-Opening Polymerization of Epoxide Monomers. *Chem. - Asian J.* **2017**, *12* (24), 3135−3140.
(63) Fox, T. G. Influence of diluent and of copolymer composition on the glass temperature of a polymer system. *Bull. Am. Phys. Soc.* **1956**, *1*, 123.
(64) Kember, M. R.; Copley, J.; Buchard, A.; Williams, C. K. Triblock copolymers from lactide and telechelic poly(cyclohexene carbonate). *Polym. Chem.* **2012**, *3* (5), 1196−1201.
(65) Vatankhah-Varnosfaderani, M.; Keith, A. N.; Cong, Y.; Liang, H.; Rosenthal, M.; Sztucki, M.; Clair, C.; Magonov, S.; Ivanov, D. A.; Dobrynin, A. V.; Sheiko, S. S. Chameleon-like elastomers with molecularly encoded strain-adaptive stiffening and coloration. *Science* **2018**, *359* (6383), 1509.

https://dx.doi.org/10.1021/jacs.9b13106
J. Am. Chem. Soc. 2020, 142, 4367−4378

(66) Arai, K.; Kotaka, T.; Kitano, Y.; Yoshimura, K. Poly(styrene-b-butadiene-b-4-vinylpyridine) Three-Block Polymers. Synthesis, Characterization, Morphology, and Mechanical Properties. *Macromolecules* **1980**, *13* (6), 1670−1678.
(67) Hashimoto, T.; Fujimura, M.; Saijo, K.; Kawai, H.; Diamant, J.; Shen, M. Strain-Induced Plastic-to-Rubber Transition of a SBS Block Copolymer and Its Blend with PS. In *Multiphase Polymers*; American Chemical Society: Washington, D.C., 1979; Vol. *176*, pp 257−275.
(68) Fujimura, M.; Hashimoto, T.; Kawai, H. Structural Change Accompanied by Plastic-to-Rubber Transition of SBS Block Copolymers. *Rubber Chem. Technol.* **1978**, *51* (2), 215−224.
(69) Chang, E. P. Viscoelastic Windows of Pressure-Sensitive Adhesives. *J. Adhes.* **1991**, *34* (1−4), 189−200.
(70) Dahlquist, C. A. Pressure-Sensitive Adhesive. In *Treatise on Adhesion and Adhesives*; Patrick, R. L., Ed.; Dekker: New York, 1969; Vol. *2*, p 219.
(71) Lee, S.; Lee, K.; Kim, Y.-W.; Shin, J. Preparation and Characterization of a Renewable Pressure-Sensitive Adhesive System Derived from ε-Decalactone, l-Lactide, Epoxidized Soybean Oil, and Rosin Ester. *ACS Sustainable Chem. Eng.* **2015**, *3* (9), 2309−2320.
(72) Ding, K.; John, A.; Shin, J.; Lee, Y.; Quinn, T.; Tolman, W. B.; Hillmyer, M. A. High-Performance Pressure-Sensitive Adhesives from Renewable Triblock Copolymers. *Biomacromolecules* **2015**, *16* (8), 2537−2539.
(73) Gallagher, J. J.; Hillmyer, M. A.; Reineke, T. M. Acrylic Triblock Copolymers Incorporating Isosorbide for Pressure Sensitive Adhesives. *ACS Sustainable Chem. Eng.* **2016**, *4* (6), 3379−3387.
(74) Shin, J.; Lee, Y.; Tolman, W. B.; Hillmyer, M. A. Thermoplastic Elastomers Derived from Menthide and Tulipalin A. *Biomacromolecules* **2012**, *13* (11), 3833−3840.
(75) Shin, J.; Martello, M. T.; Shrestha, M.; Wissinger, J. E.; Tolman, W. B.; Hillmyer, M. A. Pressure-Sensitive Adhesives from Renewable Triblock Copolymers. *Macromolecules* **2011**, *44* (1), 87−94.
(76) Wang, S.; Shuai, L.; Saha, B.; Vlachos, D. G.; Epps, T. H. From Tree to Tape: Direct Synthesis of Pressure Sensitive Adhesives from Depolymerized Raw Lignocellulosic Biomass. *ACS Cent. Sci.* **2018**, *4* (6), 701−708.
(77) Hillmyer, M. A.; Tolman, W. B. Aliphatic Polyester Block Polymers: Renewable, Degradable, and Sustainable. *Acc. Chem. Res.* **2014**, *47* (8), 2390−2396.
(78) Nasiri, M.; Saxon, D. J.; Reineke, T. M. Enhanced Mechanical and Adhesion Properties in Sustainable Triblock Copolymers via Non-covalent Interactions. *Macromolecules* **2018**, *51* (7), 2456−2465.
(79) Ding, W. Y.; Wang, S.; Yao, K. J.; Ganewatta, M. S.; Tang, C. B.; Robertson, M. L. Physical Behavior of Triblock Copolymer Thermoplastic Elastomers Containing Sustainable Rosin-Derived Polymethacrylate End Blocks. *ACS Sustainable Chem. Eng.* **2017**, *5* (12), 11470−11480.
(80) Tiu, B. D. B.; Delparastan, P.; Ney, M. R.; Gerst, M.; Messersmith, P. B. Enhanced Adhesion and Cohesion of Bioinspired Dry/Wet Pressure-Sensitive Adhesives. *ACS Appl. Mater. Interfaces* **2019**, *11* (31), 28296−28306.
(81) Brubaker, C. E.; Messersmith, P. B. The Present and Future of Biologically Inspired Adhesive Interfaces and Materials. *Langmuir* **2012**, *28* (4), 2200−2205.
(82) Jenkins, C. L.; Siebert, H. M.; Wilker, J. J. Integrating Mussel Chemistry into a Bio-Based Polymer to Create Degradable Adhesives. *Macromolecules* **2017**, *50* (2), 561−568.
(83) Hauenstein, O.; Agarwal, S.; Greiner, A. Bio-based polycarbonate as synthetic toolbox. *Nat. Commun.* **2016**, *7*, 11862.
(84) Stevens, M. P. *Polymer Chemistry: An Introduction*, 2nd ed.; Oxford University Press: New York, 1990.
(85) Yuan, Y.; Ruckenstein, E. Polyurethane toughened polylactide. *Polym. Bull.* **1998**, *40* (4), 485−490.
(86) Ellis, W. C.; Jung, Y.; Mulzer, M.; Di Girolamo, R.; Lobkovsky, E. B.; Coates, G. W. Copolymerization of CO2 and meso epoxides using enantioselective β-diiminate catalysts: a route to highly isotactic polycarbonates. *Chem. Sci.* **2014**, *5* (10), 4004.
(87) Yi, N.; Chen, T. T. D.; Unruangsri, J.; Zhu, Y.; Williams, C. K. Orthogonal functionalization of alternating polyesters: selective patterning of (AB)n sequences. *Chemical Science* **2019**, *10* (43), 9974−9980.
(88) Olsén, P.; Borke, T.; Odelius, K.; Albertsson, A.-C. ε-Decalactone: A Thermoresilient and Toughening Comonomer to Poly(l-lactide). *Biomacromolecules* **2013**, *14* (8), 2883−2890.
(89) Romero-Guido, C.; Belo, I.; Ta, T. M. N.; Cao-Hoang, L.; Alchihab, M.; Gomes, N.; Thonart, P.; Teixeira, J. A.; Destain, J.; Waché, Y. Biochemistry of lactone formation in yeast and fungi and its utilisation for the production of flavour and fragrance compounds. *Appl. Microbiol. Biotechnol.* **2011**, *89* (3), 535−547.
(90) Winkler, M.; Romain, C.; Meier, M. A. R.; Williams, C. K. Renewable polycarbonates and polyesters from 1,4-cyclohexadiene. *Green Chem.* **2015**, *17* (1), 300−306.

https://dx.doi.org/10.1021/jacs.9b13106
J. Am. Chem. Soc. 2020, 142, 4367−4378